

Dual Band-Notched Microstrip-Fed UWB Antenna for Wearable Medical Applications

F. Bahmanzadeh* and F. Mohajeri*(C.A.)

Abstract: In this article, a very small flexible antenna with dual-band rejection specifications is proposed for operating in both wearable and ultra-wideband (UWB) applications. The overall size of this antenna is about $18 \times 18 \times 0.508 \text{ mm}^3$ and by etching out two rectangular slot type single split-ring resonators (SRRs) of different dimensions from the radiating patch, dual band-notched specifications are obtained in WiMAX (3.3 GHz to 3.7 GHz) and WLAN (5.15 GHz to 5.825 GHz) wireless communication bands. The designed antenna operates over a wide impedance bandwidth ($|S_{11}| < -10 \text{ dB}$) from 2.1 GHz to 12 GHz which can cover the whole UWB band from 3.1 GHz to 10.6 GHz and reject the two mentioned bands. An asymmetrical partial ground plane and a beveled radiating patch are utilized to achieve 140% fractional bandwidth. Also, due to the good wearable radiation characteristics, this antenna can operate in industrial scientific medical (ISM) band from 2.4 GHz to 2.5 GHz. Meanwhile, the specific absorption ratio (SAR) value of the proposed antenna is less than the standard limit of 1.6 W/kg.

Keywords: Dual Band-Notched Specifications, ISM Band, UWB Antennas, Wearable Characteristics.

1 Introduction

SINCE the Federal Communication Commission (FCC) assigned unlicensed frequency range from 3.1 GHz to 10.6 GHz, UWB technology and different subsets of it such as Wireless Body Area Network (WBAN) and Wireless Personal Area Network (WPAN) has drawn lots of attention [1] hence a large number of researches have been allocated on designing UWB and wearable antennas due to their special characteristics [2, 3]. One permanent challenge in the confrontation of designing UWB antennas is the interferences between UWB spectrum from 3.1 GHz to 10.6 GHz and some existing narrowband wireless communication systems such as Worldwide

Interoperability for Microwave Access (WiMAX) from 3.3 GHz to 3.7 GHz [4], IEEE INSAT/Super-Extended C-band from 6.7 GHz to 7.1 GHz and Wireless Local Area Network (WLAN) from 5.15 GHz to 5.825 GHz [5, 6]. Therefore UWB microstrip antennas with band-notched specifications have come as a feasible solution to reduce the interferences of the mentioned systems. In addition, various methods have been used to obtain UWB antennas with single or several band-notched specifications. Etching different shapes of slots on the feed-line [7], on the radiating element [8-10] or the ground plane [11], embedding elliptical [12], circular [13] and rectangular [14] SRRs on the radiating patch, placing different shapes of strips near the feed-line [15, 16] ground plane [17] and radiating element [18] are some of these methods. Also using parasitic elements such as bended dual L-shaped branches [19] and U-shaped strips [20] is another method to achieve band-notched specifications. Microstrip UWB antennas due to their special features such as compact size, low profile, lightweight and small size, have become a noteworthy candidate in wearable applications. For instance, in [21] a wearable CPW-fed square slot antenna with an overall size of $23.5 \times 22 \times 1$

Iranian Journal of Electrical and Electronic Engineering, 2022.
Paper first received 14 December 2020, revised 24 June 2021, and accepted 06 July 2021.

* The authors are with the Department of Communications and Electronics, School of Electrical and Computer Engineering, Shiraz University, Shiraz, Iran.

E-mails: f.bahmanzadeh@shirazu.ac.ir and mohajeri@shirazu.ac.ir.

Corresponding Author: F. Mohajeri.

<https://doi.org/10.22068/IJEEE.18.1.2062>

mm³ and impedance bandwidth of 134%, and in [22] a full ground UWB arc-shaped microstrip antenna with an overall size of 80×67×3 mm³ and impedance bandwidth of 94% are proposed. Moreover, a medical wearable antenna for ISM band with Koch fractal geometry is reported in [23] with an overall size of 39×9×0.508 mm³. Although a large number of researches have been allocated on designing UWB wearable antennas and UWB band-notched antennas separately, just a few researches have been applied on designing UWB wearable antennas with band-notched specifications, which can be claimed with certainty that is a promising subject for wearable applications. For instance, a dual band-notched CPW-fed denim based wearable antenna with the total size of 43×40×2 mm³ and impedance bandwidth of 138%, and a hexagonal-shaped patch with the total size of 26×18×0.5 mm³ and impedance bandwidth of 109% are reported respectively in [24, 25].

The designed and simulated approach is based on a simple wearable antenna with dual band-notched specifications with a very small size of 18×18×0.508 mm³. The proposed antenna comprises a beveled radiator fed by a 50 Ω microstrip line and a partial ground plane printed on the bottom side of the substrate which provides a wide impedance bandwidth from 2.1 GHz to 12 GHz. Moreover, the designed antenna operates in both wearable on-body WBAN and ultra-wideband (UWB) applications, using a flexible substrate polymer-based PTFE material, commercially known as Rogers 5880 with the thickness of $h = 0.508$ mm, the dielectric constant of 2.2, and a loss tangent of about 9×10^{-4} . The technique of etching two rectangular half-wavelength slot type SRRs of various dimensions out of the patch is applied to achieve two notched bands around 3.3 GHz to 3.7 GHz for WiMAX and 5.15 GHz to 5.825 GHz for WLAN wireless communication bands. The presented antenna also resonates at 2.45 GHz, the central frequency of the ISM band for operating in medical applications. Compared to the design presented in [24], the proposed antenna has a much smaller size for operating in UWB spectrum and wider impedance bandwidth. It is good to mention that the SAR value of this antenna is less than the standard limit set by the FCC, without any special design for reducing it, such as EBG based antennas, AMC based antennas [26-28], or metamaterial wearable structures [29]. High radiation efficiency above 97%, low value of SAR, and nearly omnidirectional radiation pattern are some other good characteristics of the designed antenna.

2 Antenna Design Methodology

2.1 The Structure of the Split-Ring Resonators

The geometry of the final optimized design and position of the single rectangular slot type SRRs on it, are depicted in Fig. 1. The total length and width of the two rectangular slots directly affect the notched central

frequency and notched bandwidth respectively. The longer length means lower central frequency and the wider width means wider band-notched bandwidth. The proper length of the SRRs to filter the WiMAX and WLAN bands, can be obtained from the following design equations and the width of both slots are chosen as $a = 0.2$ mm:

$$S_n = 2 \times (W_{S_n} + L_{S_n}) - (g_n) \approx \frac{\lambda_g}{2} = \frac{c}{2f_{Notch} \sqrt{\epsilon_{eff}}} \quad (1)$$

$$\epsilon_{eff} = \frac{\epsilon_r + 1}{2} + \frac{\epsilon_r - 1}{2} \left(1 + \frac{12h}{w_f} \right)^{-2} \quad (2)$$

where S_n represents the total length of each single rectangular SRR. For $n = 1$ the structure filters WiMAX frequency band and for $n = 2$ the WLAN band rejection is obtained. L_{S_n} and W_{S_n} are the length and width of the rectangular resonators respectively, and g_n is the gaps which shown clearly in Fig. 1 (b), c is the speed of light, f_{Notch} is the notched center frequency and ϵ_{eff} is the effective dielectric constant of the substrate which is equal to 2.2 in this case.

2.2 Design Procedure of the Proposed Antenna

The presented antenna, designed in four different steps as shown in Fig. 2. The initial design is a monopole UWB antenna without any slot on it, depicts in Fig. 2(a). The radiating patch comprises a rectangular part having the size of $W_p \times L_p$ and a trapezoid shape part which printed on the top side of the Rogers 5880 flexible substrate with the size of $W \times L$, the thickness of $h = 0.508$ mm, the dielectric constant of $\epsilon_r = 2.2$, and a loss tangent of $\text{tg} \delta = 9 \times 10^{-4}$. Furthermore, a rectangular part with the size of $W_1 \times L_1$ etching out of the ground plane to improve impedance bandwidth of the antenna. To achieve 50 Ω characteristic impedance, the length and width of the microstrip feed line are chosen as $W_f \times L_f$. Antennas with single band-notched specifications are also shown in Figs. 2(b) and (c). By etching out a single rectangular slot type SRR of suitable dimensions, which

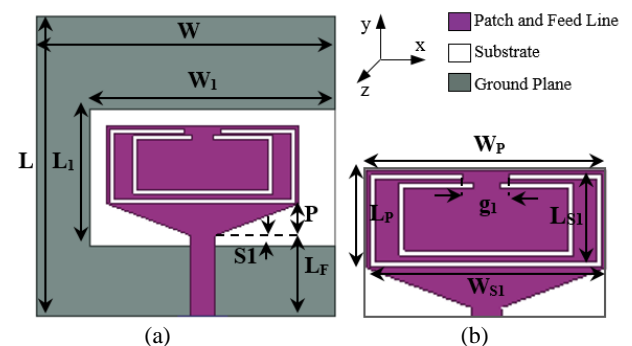


Fig. 1 a) Schematic structure of the designed dual band-notched wearable UWB antenna and b) Geometry and location of the rectangular SRR.

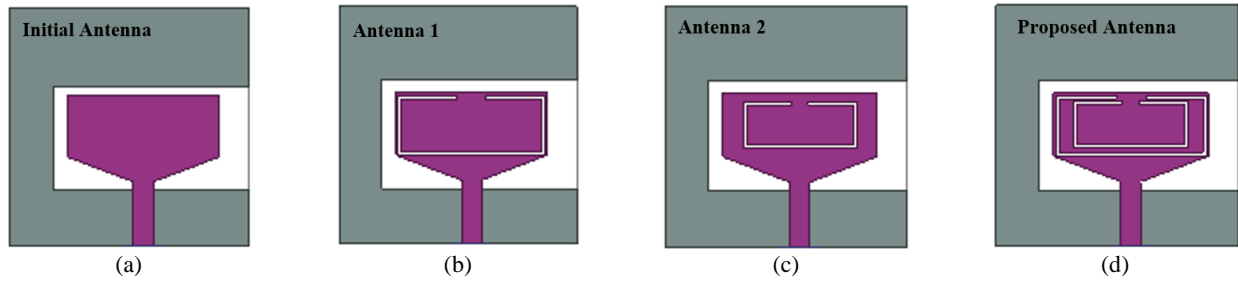


Fig. 2 Four different steps of wearable UWB antenna design: a) Initial antenna, b) Antenna with rejection of WiMAX band, c) Antenna with rejection of WLAN band, and d) Proposed UWB wearable antenna with dual band-notched specifications.

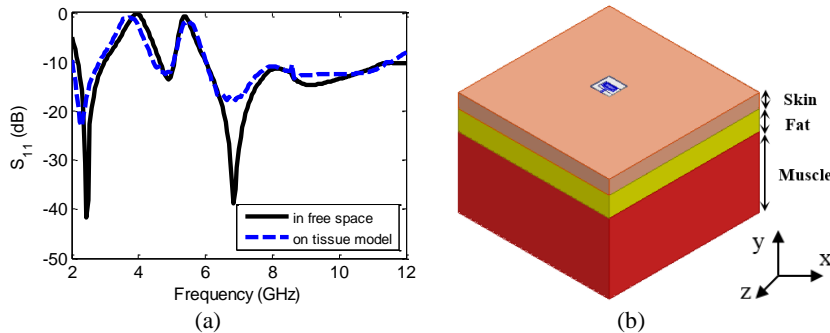


Fig. 3 a) Simulated return loss of the designed antenna in free space and on a simple human tissue model and b) Simulated human tissue model.

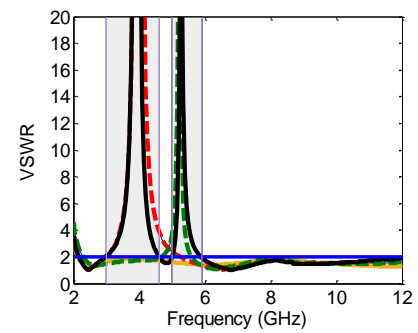


Fig. 4 Variations of VSWR versus frequency for designed stages of the antenna.

obtained from (1), symmetrically from the radiating patch, two notches at WiMAX and WLAN bands were obtained respectively having the following parameter values: $L_{s1} = 4.45$ mm, $W_{s1} = 11.2$ mm, $g_1 = 2.2$ mm, $L_{s2} = 3.5$ mm, $W_{s2} = 8.4$ mm, $g_2 = 1.25$ mm. Final design is a dual band-notched UWB wearable antenna having two slots on the radiator and operates in the wide impedance bandwidth that shown in Fig. 2(d). The radiating patch and ground plane optimum dimensions are mentioned as: $W = 18$ mm, $L = 18$ mm, $W_p = 11.5$ mm, $L_p = 4.7$ mm, $W_1 = 14.8$ mm, $L_1 = 8.25$ mm, $W_f = 1.5$ mm, $L_f = 4.85$ mm, $P = 1.9$ mm, $s_1 = 0.65$ mm.

3 Full-Wave Simulation Results

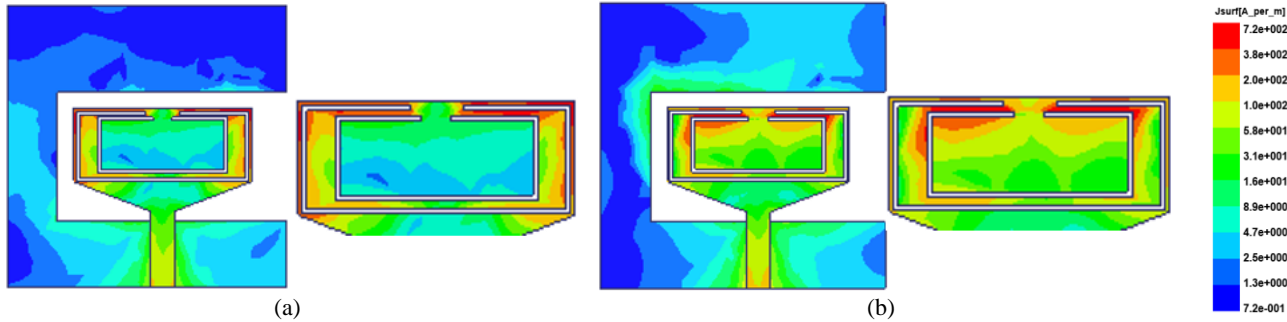
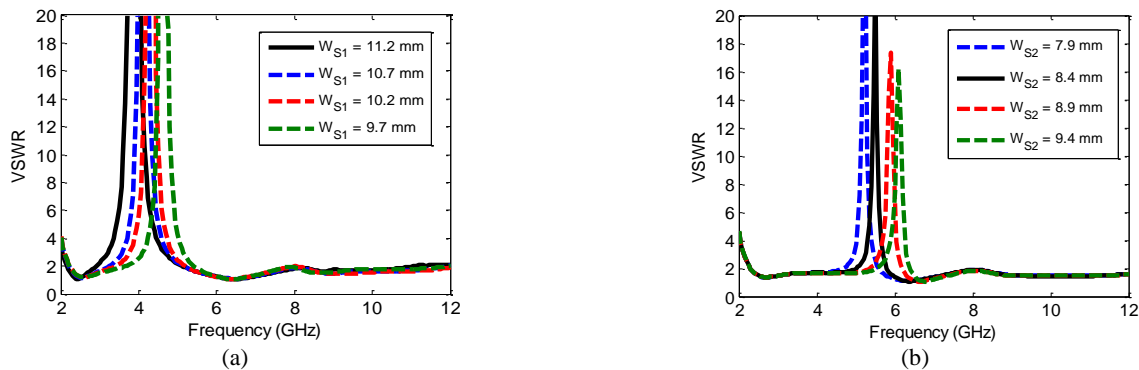
A simulator Ansoft HFSS has been utilized to calculate frequency domain parameters such as return loss, VSWR, far-field radiation patterns, gain, radiation efficiency, and surface current distribution to understand the ultra-wideband behavior of this design. The return loss of the proposed antenna in free space and in the vicinity of a simple human tissue model is shown in Fig. 3(a), which it is clear that the designed antenna operates in the frequency range from 2.1 GHz to 12 GHz ($|S_{11}|$ less than -10dB) except the two notched bands. Also, the antenna resonates at 2.45 GHz for ISM medical frequency band with $|S_{11}|$ less than -40 dB and -20 dB in free space and on the tissue model respectively. Furthermore, for SAR evaluation, a cubic human tissue model is simulated and shown in Fig. 3(b). The tissue model has an overall size of $150 \times 150 \times 70$ mm³ consist of three different layers of skin, fat, and muscle with the thickness of 3 mm, 7 mm, and 60 mm

respectively, and antenna's radiation performance examined in planar configuration at a distance of 3 mm from the mentioned human tissue model. Simulated SAR value at 2.45 GHz is obtained about 1.2 W/kg which is below the standard limit. Furthermore, the variation of VSWR versus frequency for different stages of this design is depicted in Fig. 4. As it is shown in this figure, the initial antenna (yellow curve), operates in the impedance bandwidth of about 140% from 2.1 GHz to 12GHz (VSWR<2) without incorporating any notched bands, which is noticeable due to its small dimensions. A single rectangular SRR is etched out of the radiating element in antenna 1 to decrease the interferences of WiMAX equipment from 3 GHz to 5.1 GHz covering 2100 MHz as demonstrates in Fig 4 (red curve). Similarly, another SRR is engraved into the patch for the second frequency notched band aiming to filter the WLAN frequency range from 4.6 GHz to 5.7 GHz covering about 1100 MHz (green curve). Eventually, the value of VSWR for the presented dual band-notched antenna is plotted in the black curve which is less than 2 in the frequency range from 2.1 GHz to 12 GHz except at the two notched bands from 3 GHz to 4.6 GHz and peak VSWR=113 at 3.7 GHz for WiMax and 5 GHz to 5.9 GHz, peak VSWR=25 at 5.5 GHz for WLAN and the passband is from 4.6 GHz to 5 GHz as illustrated in Fig. 4. For further description, Table 1 represents different frequency ranges of the bandwidth and rejection bands of the antenna in each step.

Simulated surface current distribution on the radiating patch and ground plane of the presented antenna, are depicted in Fig. 5 at the center frequencies of two

Table 1 Bandwidth and rejection bands of the designed antenna in each step.

	Bandwidth	WiMax bandwidth	WLAN bandwidth
Initial antenna	2.1 GHz – 12 GHz	–	–
Antenna 1	2.1 GHz – 12 GHz	3 GHz – 5.1 GHz	–
Antenna 2	2.2 GHz – 12 GHz	–	4.6 GHz – 5.7 GHz
Proposed antenna	2.1 GHz – 12 GHz	3 GHz – 4.6 GHz	5 GHz – 5.9 GHz

**Fig. 5** Distribution of surface current on the conductors of designed antenna at center resonant frequencies: a) 3.7 GHz and b) 5.5 GHz.**Fig. 6** Effect of varying dimension of single rectangular SRRs: a) Major length of outer SRR, W_{s1} , and b) Major length of inner SRR, W_{s2} .

notched bands. Fig. 5(a) depicts the distribution of surface current at 3.7 GHz for the first notched frequency. As it is clear, the flows of current are more concentrated around the outer rectangular SRR rather than the ground plane. Also, Fig. 5(b) depicts the distribution of surface current at 5.5 GHz for the second notched frequency, and similarly, it is more dominant around the smaller rectangular SRR rather than elsewhere. Generally, it can be construed that a large amount of electromagnetic energy concentration is in the vicinity of the two slots so the antenna has no radiation in the mentioned rejection bands.

To understand the effects of geometrical dimensions of the rectangular SRRs on the notched performance and impedance bandwidth, different values of W_{s1} and W_{s2} are investigated as shown in Fig. 6. $W_{s1} = 11.2$ mm and $W_{s2} = 8.4$ mm are the optimum variations that provide perfect notched bands and cover the whole WiMAX and WLAN spectrum. By increasing the length of W_{s1} from 9.7 mm to 11.2 mm, both upper and lower frequencies of the first notched band affected and shifted in the amount of about 600 MHz to the right which interfere WLAN frequency band. Similarly, by increasing W_{s2} from 7.9 mm to 3.4 GHz, second notched

band shifted in the amount of about 600 MHz to the right.

2-D radiation patterns of the proposed antenna for elevation and azimuth planes were obtained and shown in Fig. 7 at four different frequencies of 2.45 GHz, 4.8 GHz, 7 GHz, and 10.6 GHz within the bandwidth. This antenna provides a nearly omnidirectional radiation pattern in E-plane (xoz-plane) and bidirectional radiation pattern in H-plane (yoz-plane) in each frequency and also over the entire UWB spectrum. Moreover, the magnitude of cross-polarized pattern is acceptable over the impedance bandwidth in both planes.

Furthermore, Fig. 8 depicts the variation of peak gain versus frequency of the designed antenna. The very sharp notched performance of the antenna at the center frequencies of the rejection bands can be seen in this plot. Also, the peak gain is about 5.2 dBi which is significant due to the very small dimension of the antenna and the radiation efficiency of the antenna is over 97% even though the substrate is quite lossy that makes this design reasonably good compared to other previous works.

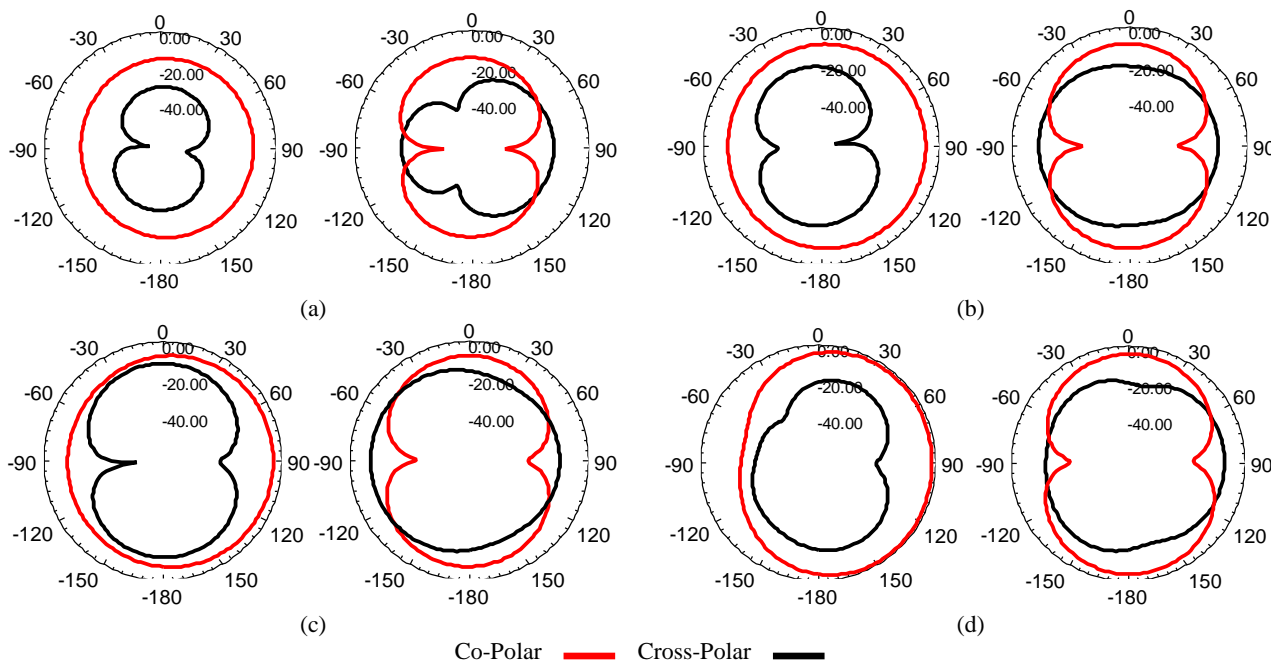


Fig. 7 2-D radiation patterns of the designed antenna in E-plane (left) and H-plane (right) at various frequencies: a) 2.45 GHz, b) 4.8 GHz, c) 7 GHz, and d) 10.6 GHz.

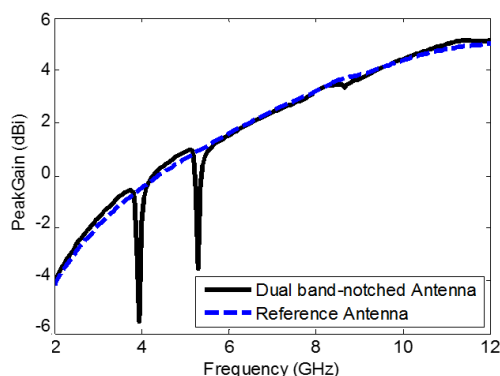


Fig. 8 Peak gain of the reference antenna and antenna with dual band-notched specifications.

4 Conclusion

This article represents a very small dual band-notched antenna for wearable 2.45 GHz ISM medical band and UWB applications. The total volume of the proposed antenna is $18 \times 18 \times 0.508 \text{ mm}^3$ covering 9.9 GHz impedance bandwidth from 2.1 GHz to 12 GHz. Other than UWB application, this antenna can also resonate in 2.45 GHz for medical frequency band and has an acceptable SAR value. Two single rectangular SRRs are applied on the radiator aiming to reject the interferences of WiMAX and WLAN bands from 3 GHz to 4.6 GHz and 5 GHz to 5.9 GHz respectively. Designed antenna shows a good behavior in far-zone and radiation patterns are quite stable considering the frequency domain results. Peak gain is about 5.2 dBi and radiation efficiency is over 97% in free space. SAR parameter evaluated over a human tissue model at 2.45 GHz with the amount of 1.2 W/kg. Consequently the proposed

antenna demonstrates a good behavior for UWB systems.

Intellectual Property

The authors confirm that they have given due consideration to the protection of intellectual property associated with this work and that there are no impediments to publication, including the timing of publication, with respect to intellectual property.

Funding

No funding was received for this work.

CRedit Authorship Contribution Statement

F. Bahmanzadeh: Idea & conceptualization, Research & investigation, Software and simulation, Revise & editing. **F. Mohajeri:** Idea & conceptualization, Revise & editing, Supervision, Analysis.

Declaration of Competing Interest

The authors hereby confirm that the submitted manuscript is an original work and has not been published so far, is not under consideration for publication by any other journal and will not be submitted to any other journal until the decision will be made by this journal. All authors have approved the manuscript and agree with its submission to "Iranian Journal of Electrical and Electronic Engineering".

References

- [1] F. C. Commission, "First report and order in the matter of version of part of 15 of the commission's rules regarding Ultra-Wideband transmission systems," *Docket 98-153 FCC 02-48*, 2002.
- [2] Y. S. Li, W. X. Li, and Q. B. Ye, "Compact reconfigurable UWB antenna integrated with SIRs and switches for multimode wireless communications," *IEICE Electronics Express*, Vol. 9, pp. 629–635, 2012.
- [3] R. Bharadwaj, C. Parini, and A. Alomainy, "Experimental investigation of 3-D human body localization using wearable ultra-wideband antennas," *IEEE Transactions on Antennas and Propagation*, Vol. 63, No. 11, pp. 5035–5044, Nov. 2015.
- [4] X. Zhang, T. L. Zhang, Y. Y. Xia, Z. H. Yan, and X. M. Wang, "Planar monopole antenna with band-notch characterization for UWB applications," *Progress In Electromagnetics Research Letters*, Vol. 6, pp. 149–156, 2009.
- [5] G. P. Gao, M. Li, S. F. Niu, X. J. Li, B. N. Li, and J. S. Zhang, "Study of a novel wideband circular slot antenna having frequency band-notched function," *Progress In Electromagnetics Research*, Vol. 96, pp. 141–154, 2009.
- [6] J. Lee, K. Kim, H. Ryu, and J. Woo, "A compact ultra wideband MIMO antenna with WLAN band-rejected operation for mobile devices," *IEEE Antennas and Wireless Propagation Letters*, Vol. 11, pp. 990–993, 2012.
- [7] C. R. Jetty and V. R. Nandanavanam, "Compact MIMO antenna with WLAN band-notch characteristics for portable UWB systems," *Progress In Electromagnetics Research C*, Vol. 88, pp. 1–12, 2018.
- [8] H. S. Mewara, M. Sharma, M. M. Sharma, and A. Dadhich, "A novel ultra-wide band antenna design using notches and stairs," in *International Conference on Signal Propagation and Computer Technology (ICSPCT 2014)*, Ajmer, pp. 425–429, 2014.
- [9] P. Gao, L. Xiong, J. Dai, S. He, and Y. Zheng, "Compact printed wide-slot UWB antenna with 3.5/5.5-GHz dual band-notched characteristics," *IEEE Antennas and Wireless Propagation Letters*, Vol. 12, pp. 983–986, 2013.
- [10] Z. H. Wu, F. Wei, X. W. Shi, and W. T. Li, "A compact quad band-notched UWB monopole antenna loaded one lateral L-Shaped slot," *Progress In Electromagnetics Research*, Vol. 139, pp. 303–315, 2013.
- [11] A. Chaabane and D. Farid, "A compact planar UWB antenna with triple controllable band-notched characteristics," *International Journal of Antennas and Propagation*, Vol. 2014, pp. 1–10, 2014.
- [12] D. Sarkar, K. V. Srivastava, and K. Saurav, "A compact microstrip-fed triple band-notched UWB monopole antenna," *IEEE Antennas and Wireless Propagation Letters*, Vol. 13, pp. 396–399, 2014.
- [13] J. Kim, C. S. Cho, and J. W. Lee, "5.2 GHz notched ultra-wideband antenna using slot-type SRR," *Electronics Letters*, Vol. 42, No. 6, pp. 315–316, 2006.
- [14] F. Bahmanzadeh and F. Mohajeri, "Simulation and fabrication of a high-isolation very compact MIMO antenna for ultra-wide band applications with dual band-notched characteristics," *International Journal of Electronics and Communications (AEU)*, Vol. 128, 2021.
- [15] T. Li, H. Zhai, G. Li, L. Li, and C. Liang, "Compact UWB band-notched antenna design using interdigital capacitance loading loop resonator," *IEEE Antennas and Wireless Propagation Letters*, Vol. 11, pp. 724–727, 2012.
- [16] V. N. Koteswara, R. Devana, and A. Maheswara Rao, "Compact UWB monopole antenna with quadruple band notched characteristics," *International Journal of Electronics*, Vol. 107, No. 2, pp. 175–196, 2019.
- [17] A. A. Ibrahim, M. A. Abdalla, and A. Boutejdar, "A printed compact band-notched antenna using octagonal radiating patch and meander slot technique for UWB applications," *Progress In Electromagnetics Research M*, Vol. 54, pp. 153–162, 2017.
- [18] W. Balani, M. Sarvagya, T. Ali, A. Samasgikar, S. Das, P. Kumar, and J. Anguera, "Design of SWB antenna with triple band notch characteristics for multipurpose wireless applications," *Applied Sciences*, Vol. 11, No. 2, p. 711, 2021.
- [19] X. L. Liu, Y. Z. Yin, P. A. Liu, J. H. Wang, and B. Xu, "A CPW-fed dual band-notched UWB antenna with a pair of bended dual-L-shape parasitic branches," *Progress In Electromagnetics Research*, Vol. 136, pp. 623–634, 2013.
- [20] J. Xu, D. Shen, G. Wang, X. Zhang, X. Zhang, and K. Wu, "A small UWB antenna with dual band-notched characteristics," *International Journal of Antennas and Propagation*, Vol. 2012, p. 656858, 2012.

- [21] S.M. Varkiani and M. Afsahi, "Compact and ultra-wideband CPW-fed square slot antenna for wearable applications," *International Journal of Electronics and Communications (AEU)*, Vol. 106, pp. 108–115, 2019.
- [22] R. B. V. B. Simorangkir, A. Kiourti, and K. P. Esselle, "UWB wearable antenna with a full ground plane based on PDMS-embedded conductive fabric," *IEEE Antennas and Wireless Propagation Letters*, Vol. 17, No. 3, pp. 493–496, Mar. 2018.
- [23] A. Arif, M. Zubair, M. Ali, M. U. Khan, and M. Q. Mehmood, "A compact, low-profile fractal antenna for wearable on-body WBAN applications," *IEEE Antennas and Wireless Propagation Letters*, Vol. 18, No. 5, pp. 981–985, 2019.
- [24] S. Chilukuri and S. Gogikar, "A CPW fed denim based wearable antenna with dual band-notched characteristics for UWB applications," *Progress in Electromagnetics Research C*, Vol. 94, pp. 233–245, 2019.
- [25] X. Guan, Z. Wang, W. Huang, B. Ren, H. Liu, P. Wen, and Y. Liu, "Novel ultra-wideband antenna with dual-band rejection characteristic for wearable applications," in *IEEE International Workshop on Electromagnetics: Applications and Student Innovation Competition (iWEM)*, Nanjing, pp. 1–3, 2016.
- [26] G. Gao, B. Hu, S. Wang, and C. Yang, "Wearable circular ring slot antenna with EBG structure for wireless body area network," *IEEE Antennas and Wireless Propagation Letters*, Vol. 17, No. 3, pp. 434–437, 2018.
- [27] B. Yin, J. Gu, X. Feng, B. Wang, Y. Yu, and W. Ruan, "A low SAR value wearable antenna for wireless body area network based on AMC structure," *Progress In Electromagnetics Research C*, Vol. 95, pp. 119–129, 2019.
- [28] A. Y. Ashyap, Z. Z. Abidin, S. H. Dahlan, H. A. Majid, S. M. Shah, M. R. Kamarudin, and A. Alomainy, "Compact and low-profile textile EBG-based antenna for wearable medical applications," *IEEE Antennas and Wireless Propagation Letters*, Vol. 16, pp. 2550–2553, 2017.
- [29] S. Yan and G. A. E. Vandenbosch, "Radiation pattern-reconfigurable wearable antenna based on metamaterial structure," *IEEE Antennas and Wireless Propagation Letters*, Vol. 15, pp. 1715–1718, 2016.



F. Bahmanzadeh was born in Shiraz, Iran, in 1996 and received her B.Sc. degree in Communication Engineering from Yasouj University in 2017, and her M.Sc. degree in Communication Engineering from Shiraz University in 2020. Her research interests include electromagnetic wave propagation and antenna design.



F. Mohajeri was born in Shiraz, Iran, in 1967 and is an Associate Professor in Communications and Electronics Engineering Department, Shiraz University. He received the B.Sc. degree in Electronics Engineering and M.Sc. degree in Communication Engineering from Shiraz University in 1991 and 1994, respectively, and Ph.D. degree in Communication Engineering from Tarbiat Modares University in 2001. He has published several technical papers and proceeding articles, and is the author of two books. His research interests include theoretical and computational electromagnetics, antennas, and electromagnetic wave interactions with special materials (chiral, metamaterial, plasma, and ...) and using of optimization methods in antenna design.



© 2022 by the authors. Licensee IUST, Tehran, Iran. This article is an open-access article distributed under the terms and conditions of the Creative Commons Attribution-NonCommercial 4.0 International (CC BY-NC 4.0) license (<https://creativecommons.org/licenses/by-nc/4.0/>).